PERIODICA POLYTECHNICA SER. MECH. ENG. VOL. 44, NO. 1, PP. 149–160 (2000)

BIFURCATION ANALYSIS OF A PIPE CONTAINING PULSATILE FLOW

Zsolt SZABÓ

Department of Applied Mechanics
Technical University of Budapest
H–1521 Budapest, Hungary
Tel: +36 1 463-1370, Fax: +36 1 463-3471
e-mail: szazs@mm.bme.hu

Received: September 30, 1999

Abstract

In this paper the dynamic behaviour of a continuum inextensible pipe containing fluid flow is investigated. The fluid is considered to be incompressible, frictionless and its velocity relative to the pipe has the same but time-periodic magnitude along the pipe at a certain time instant.

The equations of motion are derived via Lagrangian equations and Hamilton's principle. The system is non-conservative, and the amount of energy carried in and out by the flow appears in the model. It is well-known, that intricate stability problems arise when the flow pulsates and the corresponding mathematical model, a system of ordinary or partial differential equations, becomes time-periodic.

The method which constructs the state transition matrix used in Floquet theory in terms of Chebyshev polynomials is especially effective for stability analysis of systems with multi-degree-of-freedom. The implementation of this method using computer algebra enables us to obtain the boundary curves of the stable domains semi-analytically. The bifurcation analysis was performed with respect to three important parameters: the forcing frequency ω, the perturbation amplitude ν and the average flow velocity U.

Keywords: pulsatile flow, Floquet theory, Chebyshev polynomials.

1. Introduction

The equation of motion of a simply supported continuum pipe derived from *Hamilton's principle* was already discussed by HOUSNER [4] in connection with the vibrations of the Trans-Arabian pipeline. However, the correct usage of *Hamiltonian action-function* was shown by BENJAMIN [1] deriving the equation of motion of articulated pipes. SEMLER and PAÏDOUSSIS [10] have given an overview of the applicability of some numerical approaches in parametric resonances of cantilevered pipes. Several different cases of elastic pipes carrying fluid were analyzed as well (see [2], [12] and [7]).

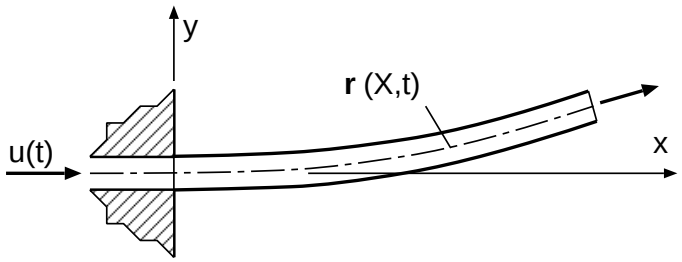

Fig. 1. Sketch of an elastic pipe with clamped-free ends

2. Description of the Model

In the following we consider a continuum elastic pipe shown in *Fig. 1*. One of its ends is attached to the wall while the other end can move freely. The motions are considered in the horizontal xy-plane. The masses per unit length of the pipe and the fluid are M and m, respectively. The upstream mass-flow $mu(t)$ is generally a periodic function of the time in the following manner:

$$u(t) = U(1 + \nu \sin \omega t)\,. \tag{1}$$

The length of the pipe is L and its axis is inextensible (i.e. the cross-sectional area of the pipe remains constant):

$$x'^2 + y'^2 = 1 \tag{2}$$

when the position vector of the pipe axis is $\mathbf{r} = \mathrm{col}\,[x(X,t),\ y(X,t)]$ and$'$ denotes $\partial/\partial X$. Hence,

$$x(X,t) = \int_0^X \sqrt{1 - y'^2(\xi,t)}\,\mathrm{d}\xi, \tag{3}$$

where X is the identifier coordinate (i.e. the arc-length) along the pipe.

Let α be the angle between the pipe and the axis x. Then

$$\cos\alpha = x' = \frac{1}{\sqrt{1+\tilde{y}'^2}} = \sqrt{1 - y'^2},$$

where $\tilde{y}(x,t) = y(X(x),t)$ is the graph of the axis in an orthogonal coordinate system, $\tilde{y}' = y'/x'$, and one can prove that $\tilde{y}'' = y''/(x')^4$ follows from the inextensibility of the pipe ($\tilde{y}'$ and $\tilde{y}''$ denote $\frac{\partial \tilde{y}}{\partial x}$ and $\frac{\partial^2 \tilde{y}}{\partial x^2}$, respectively). Thus, the curvature κ of the pipe axis is

$$\kappa = \frac{-\tilde{y}''}{\left(1+\tilde{y}'^2\right)^{\frac{3}{2}}} = \frac{-y''}{x'} \equiv \frac{-y''}{\sqrt{1-y'^2}}\,. \tag{4}$$

2.1. Equations of Motion

According to *Hamilton's principle*

$$\delta \int_{t_1}^{t_2} \{\mathcal{U} - \mathcal{T}\}\, \mathrm{d}t = \int_{t_1}^{t_2} \delta\mathcal{W}\, \mathrm{d}t, \tag{5}$$

where $\mathcal{U}$, $\mathcal{T}$ and $\delta\mathcal{W}$ are the energy of strain, the whole kinetic energy and the virtual work, respectively.

The bending moment of the beam-like pipe is a linear function of the curvature: $M_z = \kappa I_z E$. The energy of strain of a beam is

$$\mathcal{U} = \frac{I_z E}{2} \int_0^L \kappa^2\, \mathrm{d}X \approx \frac{I_z E}{2} \int_0^L y''^2 \left(1 + y'^2\right)\, \mathrm{d}X, \tag{6}$$

where the fourth degree approximation takes into account that we are investigating the stability of the trivial equilibrial shape: $y(X, t) = y'(X, t) = 0$.

Neglecting the terms of rotation (containing $\dot{\mathbf{r}}'$), we get a simple expression for the kinetic energy of the pipe and the fluid:

$$\mathcal{T} = \int_0^L \left(\frac{1}{2} M \dot{\mathbf{r}}^2 + \frac{m}{2} \left(\dot{\mathbf{r}} + u(t)\mathbf{r}'\right)^2\right) \mathrm{d}X, \tag{7}$$

where $\cdot$ ('dot') denotes $\partial/\partial t$.

The external forces changing the momentum of the flow between upstream and downstream at the ends of the pipe are

$$\mathbf{F} = -\int_0^L mu \left(\dot{\mathbf{r}} + u\mathbf{r}'\right)'\, \mathrm{d}X \equiv -mu \left[\dot{\mathbf{r}} + u\mathbf{r}'\right]_0^L \equiv \mathbf{F}_L + \mathbf{F}_0. \tag{8}$$

Thus, the virtual work of these forces is $\delta\mathcal{W} = \mathbf{F}_L \delta\mathbf{r}_L + \mathbf{F}_0 \delta\mathbf{r}_0$.

Putting the expressions of $\mathcal{U}$, $\mathcal{T}$ and $\delta\mathcal{W}$ in *Eq.* (5) we get

$$\int_{t_1}^{t_2} \int_0^L \left\{I_z E \left(y'' \delta y'' \left(1 + y'^2\right) + y''^2 y' \delta y'\right) - (M + m)\, \dot{\mathbf{r}} \delta\dot{\mathbf{r}}\right.$$

$$\left. - mu \left(\mathbf{r}' \delta\dot{\mathbf{r}} + \dot{\mathbf{r}} \delta\mathbf{r}'\right)\right\} \mathrm{d}X\, \mathrm{d}t = -\int_{t_1}^{t_2} \left[mu \left(\dot{\mathbf{r}} + u\mathbf{r}'\right) \delta\mathbf{r}\right]_0^L\, \mathrm{d}t. \tag{9}$$

After integrating by parts (excluding the term of $I_z E$) and eliminating δx one can obtain

$$\int_{t_1}^{t_2}\int_{0}^{L}\left\{I_z E\left(y''\delta y''\left(1+y'^2\right)+y''^2 y'\delta y'\right)+\delta y\left(\mathcal{G}\langle y(X,t)\rangle-\left(1+\frac{y'^2}{2}\right)y'\mathcal{G}\langle x(X,t)\rangle\right)\right.$$

$$\left.+\ \delta y\left(1+\frac{3y'^2}{2}\right)y''\int_{X}^{L}\mathcal{G}\langle x(\xi,t)\rangle\,d\xi\right\}\mathrm{d}X\,\mathrm{d}t=0, \tag{10}$$

where

$$\mathcal{G}\langle z(X,t)\rangle=(M+m)\,\ddot{z}+2mu\dot{z}'+m\dot{u}z'+mu^2z''.$$

From *Eq.* (3) one can express the derivatives of x as the function of the derivatives of y. Thus, we can eliminate all the derivatives of x from *Eq.* (10). After neglecting the fifth and higher order terms we obtain the equation of motion in dimensionless form which corresponds to the results in [9] presented by SEMLER et al.:

$$\int_{\tau_1}^{\tau_2}\int_{0}^{2}\left\{\left(y''\delta y''\left(1+y'^2\right)+y''^2y'\delta y'\right)+\delta y\left(3\ddot{y}+2\tilde{u}(\tau)\dot{y}'\left(1+y'^2\right)\right)\right.$$

$$+\delta y\left(\frac{1}{\mu}\tilde{u}^2(\tau)y''\left(1+y'^2\right)+3y'\int_{0}^{\xi}\left(\ddot{y}'y'+\dot{y}'^2\right)\mathrm{d}\eta+\frac{d\tilde{u}}{d\tau}(2-\xi)\,y''\left(1+\frac{3}{2}y'^2\right)\right)$$

$$\left.-\ \delta y\,y''\int_{\xi}^{2}\left(3\int_{0}^{\eta}\left(\ddot{y}'y'+\dot{y}'^2\right)d\tilde{\eta}+2\tilde{u}\dot{y}'y'+\frac{1}{2}\frac{d\tilde{u}}{d\tau}y'^2+\frac{1}{\mu}\tilde{u}^2y''y'\right)d\eta\right\}\mathrm{d}\xi\,\mathrm{d}\tau=0, \tag{11}$$

where

$$\mu=\frac{3m}{M+m}\,,\quad \alpha^2=I_zE\frac{\mu}{ml^4}\,,\quad \tilde{u}(\tau)=\tilde{U}(1+\nu\sin w\tau)\,,\tilde{U}=\frac{\mu}{\alpha l}U\,,$$

$$w=\frac{\omega}{\alpha}\,\tau=\alpha t\,,\quad l=\frac{L}{2}\,,\quad \xi=\frac{X}{l}\quad\text{and}\quad \tilde{y}(\xi,\tau)=\frac{1}{l}y\left(\xi l,\frac{\tau}{\alpha}\right)$$

but the 'tilde' was dropped in *Eq.* (11).

The boundary conditions are as follows:

clamped end	at $\xi=0$:	$y(0)=y'(0)=0$,
free end	at $\xi=2$:	$y''(2)=y'''(2)=0$.

2.2. Discretizing the Equation of Motion

We use *Galerkin's method* for discretizing *Eq.* (11). Assuming

$$y(\xi,\tau)=\sum_{i=1}^{n} y_i(\tau)\varphi_i(\xi), \tag{12}$$

where $\varphi_i(\xi)$ is the appropriate base function that satisfies the boundary conditions and n is the number of modes approximated by base functions. Substituting the form (12) of $y(\xi,t)$ in *Eq.* (11) the integral form will be

$$\int_{\tau_1}^{\tau_2}\delta y_i\Big\{S_{0ij}y_j+3M_{ij}\ddot{y}_j+2\tilde{u}(\tau)K_{ij}\dot{y}_j+\frac{1}{\mu}\tilde{u}^2(\tau)S_{1ij}y_j+\frac{d\tilde{u}(\tau)}{d\tau}\left(2S_{1ij}-S_{20ij}\right)y_j$$
$$+S_{01ijkl}y_jy_ky_l+3\left(M_{1ijkl}-M_{10ijkl}\right)\ddot{y}_jy_ky_l+3\left(M_{1ijkl}-M_{10ijkl}\right)\dot{y}_j\dot{y}_ky_l$$
$$+2\tilde{u}\left(K_{1ijkl}-K_{10ijkl}\right)\dot{y}_jy_ky_l+\frac{1}{\mu}\tilde{u}^2\left(S_{11ijkl}-S_{12ijkl}\right)y_jy_ky_l$$
$$+\frac{1}{2}\frac{\mathrm{d}\tilde{u}}{\mathrm{d}\tau}\left(6S_{11ijkl}-3S_{21ijkl}-K_{10ijkl}\right)y_jy_ky_l\Big\}\mathrm{d}\tau=0, \tag{13}$$

where the $\sum$-s were dropped according to Einstein's convention. Furthermore,

$$M_{ij}=\int_0^2\varphi_i\varphi_j\,\mathrm{d}\xi\ ,\quad K_{ij}=\int_0^2\varphi_i\varphi_j'\,\mathrm{d}\xi\ ,$$

$$S_{0ij}=\int_0^2\varphi_i''\varphi_j''\,\mathrm{d}\xi\ ,\quad S_{1ij}=\int_0^2\varphi_i\varphi_j''\,\mathrm{d}\xi\ ,$$

$$S_{20ij}=\int_0^2\xi\varphi_i\varphi_j''\,\mathrm{d}\xi\ ,\quad S_{01ijkl}=\int_0^2\left(\varphi_i''\varphi_j'+\varphi_i'\varphi_j''\right)\varphi_k''\varphi_l'\,\mathrm{d}\xi\ ,$$

$$K_{1ijkl}=\int_0^2\varphi_i\varphi_j'\varphi_k'\varphi_l'\,\mathrm{d}\xi\ ,\quad S_{11ijkl}=\int_0^2\varphi_i\varphi_j''\varphi_k'\varphi_l'\,\mathrm{d}\xi\ ,$$

$$S_{21ijkl}=\int_0^2\xi\varphi_i\varphi_j''\varphi_k'\varphi_l'\,\mathrm{d}\xi\ ,\quad M_{1ijkl}=\int_0^2\varphi_i\varphi_l'\int_0^\xi\varphi_j'\varphi_k'd\eta\,\mathrm{d}\xi\ ,$$

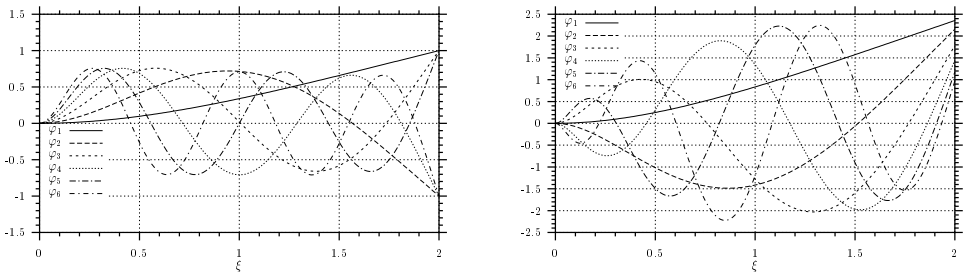

Fig. 2. Base functions from Krylov functions (left) and Chebyshev polynomials (right)

$$M_{10ijkl} = \int_0^2 \varphi_i \varphi_l'' \int_\xi^2 \int_0^\eta \varphi_j' \varphi_k' d\tilde{\eta}\, d\eta \, \mathrm{d}\xi \ , \quad K_{10ijkl} = \int_0^2 \varphi_i \varphi_l'' \int_\xi^2 \varphi_j' \varphi_k' d\eta \, \mathrm{d}\xi \ ,$$

$$S_{12ijkl} = \int_0^2 \varphi_i \varphi_l'' \int_\xi^2 \varphi_j'' \varphi_k' d\eta \, \mathrm{d}\xi \ .$$

The integral is zero for arbitrary δy_i. Hence, its coefficient (i.e. the expression in the braces in *Eq.* (13)) must be zero.

However, $\ddot{y}_j$ is also in the nonlinear terms:

$$3\left(\mathbf{M} + \left(\mathbf{M}_{1kl} - \mathbf{M}_{10kl}\right) y_k y_l\right) \ddot{\mathbf{y}},$$

where for sake of brevity we write the coefficients partially in matrix representation (instead of the indices $i,\ j$) and keeping Einstein's convention in the third and fourth indices (k, l).

If we multiply the term of $\ddot{\mathbf{y}}$ with $\mathbf{I} - \left(\mathbf{M}_{1mn} - \mathbf{M}_{10mn}\right)\mathbf{M}^{-1} y_m y_n$ we get $3\mathbf{M}\ddot{\mathbf{y}}$ where the terms of order fifth and higher were neglected.

Applying this matrix-multiplication on the other terms it yields

$$3\mathbf{M}\ddot{\mathbf{y}} + 2\tilde{u}(\tau)\mathbf{K}\dot{\mathbf{y}} + \left(\mathbf{S}_0 + \frac{1}{\mu}\tilde{u}^2(\tau)\mathbf{S}_1 + \frac{d\tilde{u}(\tau)}{d\tau}\mathbf{S}_2\right)\mathbf{y}$$

$$+3\left(\mathbf{M}_{1kl} - \mathbf{M}_{10kl}\right)\dot{\mathbf{y}}\dot{y}_k y_l + 2\tilde{u}\left(\mathbf{K}_{1kl} - \mathbf{K}_{10kl} - \tilde{\mathbf{I}}_{kl}\mathbf{K}\right)\dot{\mathbf{y}} y_k y_l$$

$$+\left(\mathbf{S}_{01kl} - \tilde{\mathbf{I}}_{kl}\mathbf{S}_0 + \frac{1}{\mu}\tilde{u}^2\left(\mathbf{S}_{11kl} - \mathbf{S}_{12kl} - \tilde{\mathbf{I}}_{kl}\mathbf{S}_1\right)\right)\mathbf{y} y_k y_l$$

$$+\frac{1}{2}\frac{\mathrm{d}\tilde{u}}{\mathrm{d}\tau}\left(6\mathbf{S}_{11kl} - 3\mathbf{S}_{21kl} - \mathbf{K}_{10kl} - 2\tilde{\mathbf{I}}_{kl}\mathbf{S}_2\right)\mathbf{y} y_k y_l = 0, \tag{14}$$

where $\quad \mathbf{y} = \left[y_j\right] \ , \quad \tilde{\mathbf{I}}_{kl} = \left(\mathbf{M}_{1kl} - \mathbf{M}_{10kl}\right)\mathbf{M}^{-1} \ , \quad \mathbf{S}_2 = 2\mathbf{S}_1 - \mathbf{S}_{20} \ .$

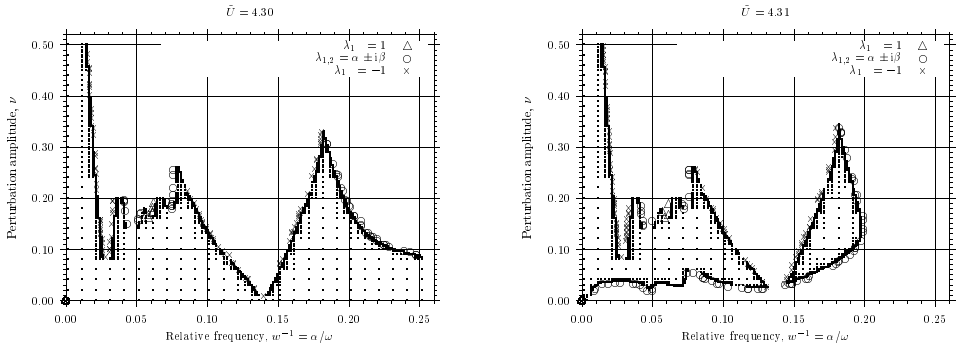

Fig. 3. Stability charts of a cantilevered pipe, $\tilde{U}_{cr} = 4.3031$ (4 Chebyshev modes)

2.3. Base Functions

Two types of base functions were used:

- at first they were searched as linear combination of *Rayleigh–Krylov functions*;
- however, the computational difficulties in obtaining the fourth-order coefficient matrices of the nonlinear part inspired the application of *Chebyshev polynomials*.

The first 6 base functions of these two types can be seen in *Fig. 2*.

Table 1. Critical values of the flow velocity $\tilde{U}$ at $\mu = 1$

n	Rayleigh–Krylov functions			Chebyshev polynomials	
	(β_n)	$\tilde{U}_{cr}$	Poincaré–Liapunov constant	$\tilde{U}_{cr}$	Poincaré–Liapunov constant
1	0.9375	∞	—	∞	—
2	2.3470	**3.3419**	–0.0805	**3.3336**	–0.351
3	3.9274	**4.2904**	–0.2752	…	…
4	5.4978	**4.2716**	–0.5367	**4.3031**	–2.307
5	7.0686	**4.2408**		**4.2614**	–2.256
6	8.6394	**4.2411**		**4.2354**	–2.221

2.3.1. Rayleigh–Krylov Functions

The following set of functions satisfies the boundary conditions of the analyzed model:

$$\varphi_i(\xi) = U(\beta_i\xi) - \frac{S(2\beta_i)}{T(2\beta_i)}V(\beta_i\xi),$$

where $S(x)$, $T(x)$, $U(x)$ and $V(x)$ are the *Krylov functions* and β_i is the root of $\cosh 2x \cos 2x = -1$ (see *Table 1*).

2.3.2. Chebyshev Polynomials

Now the base functions were constructed as follows:

$$\varphi_i(\xi) = T_{i-1}(\xi - 1) + \sum_{k=i}^{i+3} c_k T_k(\xi - 1),$$

where $T_0(x) = 1$, $T_1(x) = x$, $T_2(x) = 2x^2 - 1$, ... , $T_{r+1}(x) = 2xT_r(x) - T_{r-1}(x)$ are the *Chebyshev polynomials* and c_k-s are determined by the boundary conditions.

3. Stability Analysis

3.1. Autonomous Case

If the perturbation amplitude of the flow velocity is zero ($\nu = 0$) *Eq.* (14) will be a system of autonomous differential equations ($\tilde{u}(\tau) \equiv \tilde{U}$ and $\tilde{u}'(\tau) \equiv 0$).

Using only the first base function ($n = 1$) the system appears to be always stable. However, in case of $n > 1$ a critical value of $\tilde{U}$ appears above which the system loses its asymptotically stable behaviour and becomes unstable.

At this critical value $\tilde{U}_{cr}$ a pair of pure imaginary roots cross the imaginary axis, i.e. *Hopf bifurcation* occurs.

In *Table 1* the critical values of $\tilde{U}$ are listed w.r.t. the number of base functions n and their types. In each case the system is stable below these values ($0 < \tilde{U} < \tilde{U}_{cr}$).

Because of the symmetric nonlinearities (there isn't any second order term) the plane of the critical eigenvectors approximates the centre manifold in second order. Hence, the centre manifold reduction can be done easily. The bifurcation analysis results negative *Poincaré–Liapunov constants*, i.e. *super-critical Hopf bifurcation* takes place in these cases that was verified by simulations.

3.2. Non-autonomous Case

3.2.1. Linear Analysis

The discretized equation of motion (14) can be written as a first order system of ordinary differential equations:

$$\dot{\mathbf{x}} = \mathbf{A}(\tau)\mathbf{x} + \begin{bmatrix} \mathbf{0} \\ \mathbf{M}^{-1}\mathbf{f}(\tau, \mathbf{x}) \end{bmatrix}. \tag{15}$$

It is well-known from *Floquet theory* (see e.g. [3]) that the stability of a system like (15), where the linear part is periodic ($\mathbf{A}(\tau + T) = \mathbf{A}(\tau)$, $T = 2\pi w^{-1}$), is determined by the characteristic multipliers (i.e. the eigenvalues of the *Floquet Transition Matrix* $\mathbf{C} = \Phi(T)$, where $\Phi(\tau)$ is the *State Transition Matrix*: $\dot{\Phi} = \mathbf{A}\Phi$ and $\Phi(0) = \mathbf{I}$ is the identity matrix). SINHA and WU [11] have developed a numerical method for stability analysis in any general case based on *Chebyshev polynomials*. If we present the solution vector as an expansion of these polynomials we obtain a set of linear algebraic equations from the differential equations. The solution of this system gives the coefficients of the Chebyshev expansion. In this way we obtain an approximation of the *Floquet Transition Matrix* $\mathbf{C}$ and we can analyze the characteristic multipliers $\lambda_i(\mathbf{C})$ at particular system parameters. The linear system is asymptotically stable iff all the multipliers are located in the open unit disk of the complex plane. Fixing the parameters of our mechanical structures and choosing $\tilde{U}$, ν and w for bifurcation parameters, Sinha's numerical method provides the stability domains of the system.

Figs. 3 and *4* show slices of the three dimensional $(\tilde{U}, w, \nu)$ theoretical stability domain around the critical value $\tilde{U}_{cr}$ determined in Section 3.1. The dotted region represents the stable domain of the analyzed space. The symbols on the boundary show the type of stability loss, i.e. the way where the characteristic multipliers leave the unit disk while crossing the stability boundary.

It is worth noticing that the stability charts in *Fig. 4* have more complicated structure for low values of α/ω. Thus, one should consider applying more base functions in this region to describe the exact behaviour of the model.

3.2.2. Nonlinear Analysis

In order to be able to perform the stability investigations of the nonlinear system (15) we follow the procedure described in [8]. Let us define the $2T$ periodic *Liapunov–Floquet transformation*:

$$\mathbf{P}(\tau) = \Phi(\tau)e^{-\tau\mathbf{R}},$$

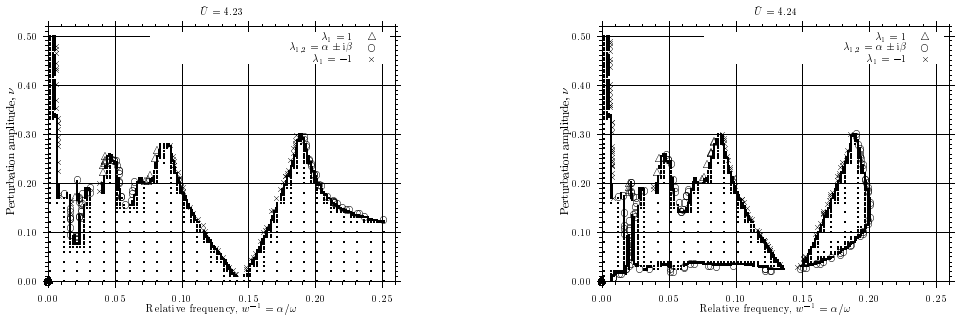

Fig. 4. Stability charts of a cantilevered pipe, $\tilde{U}_{cr} = 4.2354$ (6 Chebyshev modes)

where $\Phi(\tau)$ is the *State Transition Matrix* and $\exp(2T\mathbf{R}) = \mathbf{C}^2$. Substitution of $\mathbf{x} = \mathbf{P}(\tau)\mathbf{Tz}$ in *Eq.* (15) results a constant coefficient matrix in the linear term:

$$\dot{\mathbf{z}} = \mathbf{T}^{-1}\mathbf{RTz} + \mathbf{T}^{-1}\mathbf{P}^{-1}(\tau)\begin{bmatrix} \mathbf{0} \\ \mathbf{M}^{-1}\mathbf{f}(\tau, \mathbf{P}(\tau)\mathbf{Tz}) \end{bmatrix}. \tag{16}$$

If $\mathbf{T}$ is the matrix of eigenvectors of $\mathbf{R}$ then the coefficient matrix of the linear term is in *Jordan form* where the stable and unstable manifolds can be separated. As $\mathbf{P}(\tau)$ is a periodic function of τ with principal period $2T$, it can be expanded in *Fourier series*. Substituting this expansion in the nonlinear term and doing some trigonometrical simplifications we can easily separate the constants and the time-dependent terms. Because of the symmetric nonlinearities the center manifold reduction is trivial and we have to follow the same procedure described at the end of Section 3.1.

The bifurcation analysis was performed at some typical points in plane $\tilde{U} = 4.31$ where line $\nu = 0.15$ crosses the curves of the stability boundary. The results of the analysis are summarized in *Table 2*.

One can notice that *flip* ($N = 1, 2, 9, 10$) and *fold* ($N = 5, 6$) bifurcations bounded unstable regions alternate each other with *Hopf* bifurcation bounded regions ($N = 3, 4, 7, 8$) in between. On the right-most boundary ($N = 11$) and at the bottom ($N = 12$) *Hopf* bifurcation can be observed. The bifurcation analysis yielded negative *Poincaré–Liapunov constants* that means *super-critical* bifurcations occur. However, at points 2,6 and 10 the centre manifold has positive coefficient in the nonlinear term, i.e. *subcritical flip* and *fold* bifurcations take place at these points, respectively. *Fig. 5* shows a bifurcation diagram at $(\tilde{U}, \nu) = (4.31, 0.15)$ changing the value of w^{-1} from 0.024 to 0.028 by 10^{-4}. On the vertical axis are the values of $\dot{y}_4(t)$ acquired with the frequency corresponding to the principal period $1/T$. At the beginning, the *flip bifurcation* can be seen ($2T$ periodic solution), and after $w^{-1} = 0.0251$ it goes through a *Hopf bifurcation* with period something greater than $10T$. The period of the solution decreases

Table 2. Overview of some critical points (at $\mu = 1$ and $\tilde{U} = 4.31$)

N	ν	w^{-1}	λ_{cr} ($\alpha^2 + \beta^2 = 1$)	bif. type	P–L constant
1	0.15	**0.0238963**	–1	flip	**–236.9**
2	0.15	**0.0331140**	–1	flip	82.14
3	0.15	0.0428920	$\alpha \pm \mathrm{i}\beta$	Hopf	*–9.320*
4	0.15	0.0505600	$\alpha \pm \mathrm{i}\beta$	Hopf	*–0.058*
5	0.15	**0.0565510**	1	fold	**–44.82**
6	0.15	**0.0602135**	1	fold	31.69
7	0.15	0.0733880	$\alpha \pm \mathrm{i}\beta$	Hopf	*–1.981*
8	0.15	0.0757590	$\alpha \pm \mathrm{i}\beta$	Hopf	*–1.839*
9	0.15	**0.0974200**	–1	flip	**–8.125**
10	0.15	**0.1620620**	–1	flip	2.673
11	0.15	0.1976700	$\alpha \pm \mathrm{i}\beta$	Hopf	**–2.390**
12	0.033	0.1	$\alpha \pm \mathrm{i}\beta$	Hopf	*–3.915*

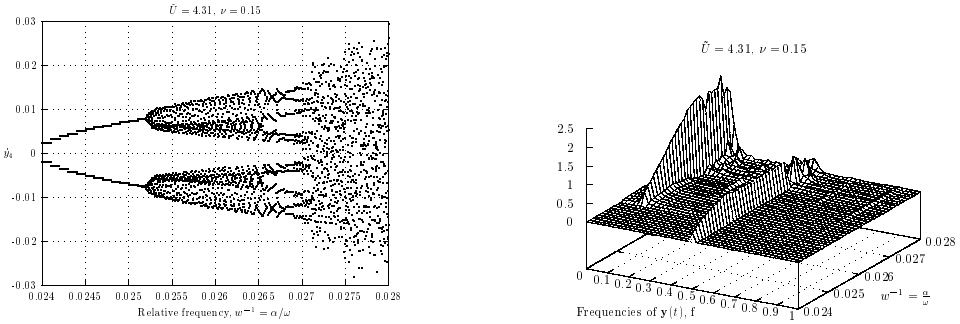

Fig. 5. Bifurcation and waterfall diagrams

slightly, and when it equals $10T$ a sequence of period doubling follows (before $w^{-1} = 0.027$). And finally the chaotic behaviour appears.

All of these can be observed on the waterfall diagram on the right side of *Fig. 5*: the peak in spectrum at $f = 0.5$, the other peak around $f = 0.1$ that refers to the *Hopf bifurcation*, and the "noise" of chaotic solution when $w^{-1} > 0.027$.

4. Conclusions

Equations of motion of a cantilevered pipe were derived via *Lagrangian equations* and *Hamilton's principle*. Nonlinear stability analyses were performed both in autonomous and time-periodic case. The stability charts show that the harmonic

perturbation of the fluid velocity with certain values of ν and w can destabilize the equilibrium of the pipe even for $\tilde{U} < \tilde{U}_{cr}$ as also pointed out by PAÏDOUSSIS in [5] and [6]. On the other hand, the fact that appropriate harmonic perturbation can stabilize otherwise unstable equilibria, it may be very useful when great fluid mass has to be transported in thin elastic pipes.

The numerical method based on the *Chebyshev polynomials* is very powerful in the case of the analysis of continuum pipe models. Discretization of *Eq.* (11) results finite system with many degrees of freedom. The numerical calculations show different stability charts depending on the number of modes sensitively.

The bifurcation analysis shows that stable T and $2T$ periodic solutions are on the left side of the unstable regions bounded by *fold* and *flip bifurcations*, respectively. In case of *Hopf bifurcations* the solutions converge to a stable torus. An unstable region bounded by flip bifurcations was scrutinized by numerical simulations and its bifurcation and waterfall diagrams were created. This investigation shows the presence of chaotic solutions. Further simulations should be carried out to get more information about the nonlinear behaviour of solutions in the other unstable regions.

Acknowledgement

This research was partially supported by MKM/FKFP-0380 and the Hungarian Scientific Research Foundation OTKA Grant No. F-030378.

References

[1] BENJAMIN, T. B.: Dynamics of System of Articulated Pipes Conveying Fluid, I-II. *Proceedings of the Royal Society of London.* Series, A261, pp. 457–499, 1961.
[2] BLEVINS, R. D.: Flow-Induced Vibration, Van Nostrand Reinhold, New York, 1990.
[3] FARKAS, M.: Periodic Motions, Springer-Verlag, New York, 1994.
[4] HOUSNER, G. W.: Bending Vibrations of a Pipe Line Containing Flowing Fluid, *Journal of Applied Mechanics*, **19**, pp. 205–208, 1952.
[5] PAÏDOUSSIS, M. P. – SUNDARARAJAN, C.: Parametric and Combination Resonances of a Pipe Conveying Pulsating Fluid, *Journal of Applied Mechanics*, **42**, No. 4, pp. 780–784, 1975.
[6] PAÏDOUSSIS, M. P. – ISSID, N. T.: Experiments on Parametric Resonance of Pipes Containing Pulsatile Flow, *Journal of Applied Mechanics*, Vol. 98, No. 2, pp. 198–202, 1976.
[7] PAÏDOUSSIS, M. P. – LI, G. X.: Pipes Conveying Fluid: A Model Dynamical Problem, *Journal of Fluids and Structures*, **7**, pp. 137–204, 1993.
[8] PANDIYAN, R. – SINHA, S. C.: Analysis of Time-Periodic Nonlinear Dynamical Systems Undergoing Bifurcations, *Nonlinear Dynamics*, **8**, pp. 21–43, 1995.
[9] SEMLER, C. – LI, G. X. – PAÏDOUSSIS, M. P.: The Non-linear Equations of Motion of Pipes Conveying Fluid, *Journal of Sound and Vibration*, **169**, No. 5, pp. 577–599, 1994.
[10] SEMLER, C. – PAÏDOUSSIS, M. P.: Parametric Resonances of a Cantilevered Pipe Conveying Fluid: A Nonlinear Analysis, *ASME/Design Engineering Technical Conferences*. DE-Vol.84-1, Vol. 3, Part A, pp. 325–331, 1995.
[11] SINHA, S. C. – WU, D.-H., An Efficient Computational Scheme for the Analysis of Periodic Systems, *Journal of Sound and Vibration*, **151**, pp. 91–117, 1991.
[12] TROGER, H., Nonlinear Stability and Bifurcation Theory: An Introduction for Engineers and Applied Scientists, Springer-Verlag, Wien, 1991.